




Immunoinformatics and molecular dynamics studies to predict T-cell-specific epitopes of four *Klebsiella pneumoniae* fimbriae antigens

Mosayeb Rostamian , Alireza Farasat , Roya Chegene Lorestani , Fatemeh Nemati Zargaran , Keyghobad Ghadiri & Alisha Akya

To cite this article: Mosayeb Rostamian , Alireza Farasat , Roya Chegene Lorestani , Fatemeh Nemati Zargaran , Keyghobad Ghadiri & Alisha Akya (2020): Immunoinformatics and molecular dynamics studies to predict T-cell-specific epitopes of four *Klebsiella pneumoniae* fimbriae antigens, Journal of Biomolecular Structure and Dynamics, DOI: [10.1080/07391102.2020.1810126](https://doi.org/10.1080/07391102.2020.1810126)

To link to this article: <https://doi.org/10.1080/07391102.2020.1810126>

 View supplementary material [↗](#)

 Published online: 21 Aug 2020.


 Submit your article to this journal [↗](#)

 View related articles [↗](#)

 View Crossmark data [↗](#)



Immunoinformatics and molecular dynamics studies to predict T-cell-specific epitopes of four *Klebsiella pneumoniae* fimbriae antigens

Mosayeb Rostamian^a , Alireza Farasat^b, Roya Chegene Lorestani^a, Fatemeh Nemati Zargaran^a, Keyghobad Ghadiri^a and Alisha Akya^a

^aInfectious Diseases Research Center, Health Institute, Kermanshah University of Medical Sciences, Kermanshah, Iran; ^bCellular and Molecular Research Center, Qazvin University of Medical Sciences, Qazvin, Iran

Communicated by Ramaswamy H. Sarma

ABSTRACT

Klebsiella pneumoniae (*K. pneumoniae*) is a causative agent of severe infections in humans. There is no publically available vaccine for *K. pneumoniae* infections yet. Here, using comprehensive immunoinformatics methods, T-cell-specific epitopes of four type 1 fimbriae antigens of *K. pneumoniae* were predicted and evaluated as potential vaccine candidates. Both CD8⁺ (class I) and CD4⁺ (class II) T-cell-specific epitopes were predicted and the epitopes similar to human proteome were excluded. Subsequently, the windows of class-II epitopes containing class-I epitopes were determined. The immunogenicity, IFN- γ production and population coverage were also estimated. Using the 3D structure of HLA and epitopes, molecular docking was carried out. Two best epitopes were selected for molecular dynamics studies. Our prediction and analyses resulted in the several dominant epitopes for each antigen. The docking results showed that all selected epitopes can bind to their restricted HLA molecules with high affinity. The molecular dynamics results indicated the stability of system with minimum possible deviation, suggesting the selected epitopes can be promising candidates for stably binding to HLA molecules. Altogether, our results suggest that the selected T-cell-specific epitopes of *K. pneumoniae* fimbriae antigens, particularly the two epitopes confirmed by molecular dynamics, can be applied for vaccine development. However, the *in vitro* and *in vivo* studies are required to authenticate the results of the present study.

Abbreviations: ANN: Artificial neural network; Comblib: Combinatorial peptide libraries; CPORT: Consensus prediction of interface residues in transient complexes; HLA: Human leukocyte antigen; MD: Molecular dynamics; RMSD: Root mean square deviation; RMSF: Root mean square fluctuation; SMM: Stabilized matrix method; TIP3P: Transferable intermolecular potential with 3 points

ARTICLE HISTORY

Received 13 May 2020
Accepted 10 August 2020

KEYWORDS

Klebsiella pneumoniae;
vaccine; immunoinformatics;
type 1 fimbriae; T-cell-
specific epitope;
molecular dynamics

1. Introduction

Klebsiella pneumoniae is a Gram-negative bacterium that resides in the environment (soil, water, etc.) and the gastrointestinal tract of mammals including humans. In humans, it can cause infection if gains entry to the blood circulation and other sterile tissues (Piperaki et al., 2017).

Various approaches have been tested to combat the antimicrobial resistance related problems in pathogenic bacteria including the recent progress in bioinformatics which has provided novel tools to identify potential drug targets (Miriyala et al., 2018; Sugumar et al., 2014). However, the emergence of strains resistant to various antibiotics by presenting several resistance mechanisms as well as the hyper-virulent strains greatly narrow down the therapeutic options for *K. pneumoniae* infections. Consequently, this problem has attracted a great attention for vaccine development (Malathi et al., 2019; Miriyala et al., 2020; Piperaki et al., 2017).

The development of an effective vaccine would be a great help to control the *K. pneumoniae* infections. Due to the safety concern, whole cell vaccines that consist of multiple proteins are not considered as perfect vaccines. On the other hand, no completely effective single antigen candidate has been found so far for *K. pneumoniae* and attempts for finding a good vaccine candidate are still ongoing.

Four virulence factors of *K. pneumoniae* have been well characterized, namely fimbriae, lipopolysaccharide, capsule, and siderophores. These virulence factors assist this opportunistic pathogen to circumvent the host immune defenses (Paczosa & Meccas, 2016; Shon et al., 2013). Type 1 and type 3 fimbriae in *K. pneumoniae* facilitate adherence to biotic and abiotic surfaces and mediate epithelial cell invasion and biofilm formation (Piperaki et al., 2017). Type 1 fimbriae composed of a tip fibrillum connected to the rod. Tip fibrillum is composed of a single copy of FimH (the adhesion) and a single copy of FimG (the tip subunit) proteins connected to the

Table 1. Alleles used for epitope prediction.

Class-I alleles	Presence in			Class-II alleles	Presence in		
	SYFPEITHI	ProPredI	IEDB		SYFPEITHI	ProPredII	IEDB
HLA-A*01:01	+	+	+	HLA-DRB1*03:01	+	+	+
HLA-A*02:01	+	+	+	HLA-DRB1*07:01	+	+	+
HLA-A*03:01	+	+	+	HLA-DRB1*15:01	+	+	+
HLA-A*11:01	+	+	+	HLA-DRB3*01:01	-	-	-
HLA-A*24:02	+	+	+	HLA-DRB3*02:02	-	-	-
HLA-A*30:01	-	-	+	HLA-DRB4*01:01	-	-	-
HLA-A*68:02	-	-	+	HLA-DRB5*01:01	-	+	+
HLA-B*08:01	+	+	+				
HLA-B*35:01	+	+	+				
HLA-B*51:01	+	+	+				

rod via the FimF protein (the adaptor subunit). The rod is made up of over 1000 copies of FimA (the major subunit) proteins (Volkan et al., 2014). It has been shown that the major structural proteins of fimbriae are effective immunogens (Staniszewska et al., 2000; Witkowska et al., 2005). Fimbriae (especially type 3) has been shown to mediate immunity to *K. pneumoniae* infection in murine models *in vivo* and *in vitro* (Babu et al., 2017; Lavender et al., 2005; Li et al., 2010). However, vaccine candidates based on fimbriae and other virulence factors in *K. pneumoniae* are at early phases of development and need more studies (Choi et al., 2019).

Reverse vaccinology and peptide mapping via immunoinformatics approaches are widely used strategies for vaccine development (Rappuoli et al., 2016). Since evaluation of individual vaccines under *in vivo* conditions is an enduring task, bioinformatics approaches can offer an alternative, attractive, cost-effective, and much easier way to evaluate antigens and their more potent parts (epitopes) as vaccine candidates (Kazi et al., 2018). Moreover, molecular dynamics (MD) simulations that can evaluate the dynamic behavior of molecular systems (Bai & Yao, 2016) can be applied to find the best epitopes as vaccine candidates. MD can explore the interactions between epitopes and receptors (as protein–ligand complexes) as well as conformational changes of the receptors at the atomic level (Bello & Correa-Basurto, 2013; Chen et al., 2016; Knapp et al., 2015; Mirza et al., 2016; Singaravelu et al., 2014).

Instead of whole protein antigens, the most potent parts of them (epitopes) have been suggested as vaccine due to cost-effective and efficacy. T-cell-specific epitopes are short length amino acid sequences that can induce desirable, specific, and broad-spectrum T-cell-dependent immunity (Chyau Liang, 1998). It has been shown that T-cell-dependent immunity is important to induce full protection against *K. pneumoniae*, although its roles remain to be more clarified (Choi et al., 2019; Lee et al., 2015).

Immunoinformatics approaches are useful in predicting immunogenic epitopes as vaccine candidates and are widely accepted in many scientific fields (Swetha et al., 2016). In the present study, considering T-cell-dependent immune responses, T-cell-specific epitopes of four proteins of type 1 fimbriae namely FimA, FimF, FimG and FimH were found and investigated using accurate immunoinformatics, docking and molecular dynamics approaches.

2. Methods

2.1. Preparation of protein sequences

Four proteins of type 1 fimbriae, namely FimA, FimF, FimG and FimH were selected. In spite of FimF, FimG, and FimH presented as single proteins, FimA is a subunit of identical proteins that assemble and form the rod part of the fimbriae. The amino acid sequences of four Fim proteins were obtained from NCBI protein database (<https://www.ncbi.nlm.nih.gov/protein>) with the following accession numbers: FimA (CDO12578.1), FimF (CDO12574.1), FimG (CDO12573.1), and FimH (CDO12572.1).

2.2. CD8+ T-cell epitope (class I) prediction

CD8+ T-cell epitopes bind to human leukocyte antigen (HLA)-I alleles. The HLA alleles need to be defined by the epitope prediction tools. Therefore, first, 10 highly frequent HLA-I alleles in the world population were obtained from the allele frequency net database (<http://www.allelefrequencies.net> (Gonzalez-Galarza et al., 2015)) (Table 1). These alleles were also present in top 27 frequent alleles presented in IEDB prediction tool (Fleri et al., 2017).

At the next step, based on the 10 frequent HLA-I alleles, four Fim protein sequences were screened individually using three different MHC-I prediction applications, namely IEDB (<http://tools.iedb.org> (Fleri et al., 2017)), SYFPEITHI (<http://www.syfpeithi.de/bin/MHCServer.dll/EpitopePrediction.htm> (Schuler et al., 2007)), and Pro-PredI (<http://crdd.osdd.net/raghava/propred1/> (Singh & Raghava, 2003)), according to the previously works with some modifications (Akyu et al., 2019; Dikhit et al., 2016; Prasasty et al., 2019). The thresholds were set as the tools default (≤ 1 percentile rank for IEDB and ≥ 10 score for SYFPEITHI and ProPredI). Only 9-mer epitopes were predicted because for class-I epitopes, the binding groove accommodates short length (usually 9-mer) amino acids (Gfeller et al., 2018).

All predicted 9-mer epitopes were clustered and aligned to find epitopes with sequence similarity using Clustal Omega multiple sequence alignment tool (Li et al., 2015) and IEDB Epitope Cluster Analysis tool (<http://tools.iedb.org/cluster/>). The cutoff was set at $\geq 70\%$ similarity. To reduce the number of predicted epitopes, only one epitope per cluster was selected which was the epitope with the highest scores achieved by the prediction tools or the epitope that had been predicted by at least two out of three prediction tools.

The immunogenicity of each selected epitope was also evaluated using IEDB Class-I immunogenicity tool (<http://tools.iedb.org/immunogenicity/>) that used the position and the properties of amino acids to predict the epitope immunogenicity (Calis et al., 2013).

2.3. CD4+ T-cell epitope (class II) prediction

CD4+ T-cell epitopes bind to HLA-II alleles. The epitope prediction tools need defining these HLA alleles to predict epitopes. In the present study, seven highly frequent HLA-II alleles in the world population presented by IEDB prediction tool (Fleri et al., 2017) were used (Table 1).

Based on defined HLA-II alleles, class-II epitopes of four Fim proteins were predicted by three MHC-II prediction applications, IEDB, SYFPEITHI, and ProPredII (<http://crdd.osdd.net/raghava/propred/>) according to the tools recommendations and previous works (Panahi et al., 2018; Prasasty et al., 2019). The thresholds were set on ≤ 10 percentile rank for IEDB and ≥ 10 score for SYFPEITHI and ProPredII. Only 15-mer epitopes were predicted. Note that of seven HLA-II alleles selected, only three and four alleles existed in SYFPEITHI and ProPredII tools, respectively (Table 1).

All predicted 15-mer epitopes were clustered and aligned and the best epitopes were selected as previously mentioned (see Section 2.2). Finally, the ability of the selected epitopes in interferon gamma (IFN- γ) production was evaluated using IFNepitope server (<http://crdd.osdd.net/raghava/ifnepitope/>).

2.4. Human similarity exclusion and searching experimental records

Using BLASTP (<https://blast.ncbi.nlm.nih.gov/Blast.cgi?PAGE=Proteins>) all selected class-I and II epitopes were screened for homology with human proteome (taxid 9606, the default human proteome in NCBI) and those with more than 90% similarity (for both identity and coverage values in BLASTP) were excluded from the study.

Using the home page of IEDB (<https://www.iedb.org/>), the selected epitopes were investigated for experimental records by applying each epitope as a query and selecting human as the host. Furthermore, to double check the results, all four Fim antigens were investigated for experimental records using PubMed website and the IEDB home page.

2.5. Finding class-II epitopes containing class-I epitopes

Knowing that 9-mer class-I epitopes can be windows of 15-mer class-II epitopes, all predicted class-I epitopes were aligned with the predicted class-II epitopes to find these windows. For this purpose, all class-I and II epitopes were clustered using IEDB Epitope Cluster Analysis tool with cutoff set at $\geq 70\%$ similarity. The class-II epitopes that contained at least one class-I epitope were selected for further studies. The class-I epitopes which were windows of class-II epitopes were also kept for further analysis.

2.6. Final selected T-cell epitopes

For each Fim antigen, five best class-II epitopes were selected based on the following criteria: (1) The epitope contained more class-I epitopes, (2) The epitope with higher prediction scores, (3) The epitope predicted by more prediction tools, and (4) The epitope predicted positive in IFN- γ production. Similarly, the five best class-I epitopes of each Fim antigen were selected based on the following criteria: (1) The epitope was a window of a high score class-II epitope, (2) The epitope with higher prediction scores, (3) The epitope predicted by more tools, and (4) The epitope with higher immunogenicity score.

2.7. Prediction of population coverage

Since HLA molecules are polymorph in the human population, the HLA-restricted epitopes as vaccine candidates should cover a large proportion of the population. To predict the population coverage of final HLA-epitopes combination, IEDB population coverage analysis tool (http://tools.iedb.org/tools/population/iedb_input (Bui et al., 2006), was used. Although *K. pneumoniae* infections have been frequently reported worldwide, to make the issue simple, seven countries with reported Carbapenemase-producing *K. pneumoniae* (Munoz-Price et al., 2013) were selected as template and entered to the IEDB population coverage analysis tool. Final epitopes and alleles were also entered to the tool and the rest of the parameters remained as default.

2.8. Tertiary structures of HLA molecules and T-cell epitopes

The final selected class-I epitopes were restricted to six HLA-I alleles. The crystal structure of these alleles was downloaded from PDB databank with the following PDB IDs: HLA-A*01:01 (ID: 6AT9), HLA-A*02:01 (ID: 5HHP), HLA-A*03:01 (ID: 3RL1), HLA-A*24:02 (ID: 3I6L), HLA-B*35:01 (ID: 2CIK) and HLA-B*51:01 (ID: 1E27).

The final class-II epitopes were all restricted to one HLA-II allele (HLA-DRB1*15:01). The crystal structure of this allele was also obtained from PDB databank (PDB ID: 1BX2).

The 3D structures of the final epitopes were modeled by PEP-FOLD server (Shen et al., 2014; Thevenet et al., 2012) that predicted five most demonstrable models for each epitope. The PDB format of the model with the lowest energy was downloaded for further analysis.

The modeled tertiary structure of epitopes was validated by generation of Ramachandran plot using RAMPAGE server (<http://mordred.bioc.cam.ac.uk/~rapper/rampage.php> (Lovell et al., 2003)). Ramachandran plotting was used to predict the possibility of epitope amino acids to form a secondary structure based on dihedral angles. The qualities of modeled tertiary structures were assessed based on the percentage of the amino acid residues in the favored, allowed and outlier regions (Lovell et al., 2003).

2.9. Molecular docking studies

For exactly predicting which active and passive residues would be incorporated in the docking interactions, consensus prediction of interface residues in transient complexes (CPORT) (<https://milou.science.uu.nl/services/CPORT/>) was applied (de Vries & Bonvin, 2011). After collecting these residues for involved structures, HADDOCK 2.2 (<http://haddock.science.uu.nl/services/HADDOCK2.2>) was applied to carry out the docking simulations for the tertiary structures of HLA alleles and epitopes. The server presented the results as docking scores along with other parameters (Dominguez et al., 2003; van Zundert et al., 2016).

2.10. Molecular dynamics simulations (MD)

A class-II epitope of FimG antigen and its residing class-I epitope which were the best epitopes based on our immunoinformatics and docking evaluations, were selected for MD simulation studies. The combination of these class-II and I epitopes and their restricted HLAs was studied through MD simulation using CHARMM36 force field of GROMACS, v5.1 (Gheibi et al., 2020). The dimensions of cubic box for MD simulation were selected so that each atom of the receptor was at least 10 Angstrom away from walls of the cubic box. Transferable intermolecular potential with 3 points (TIP3P) water model was applied to fill the system (Gheibi et al., 2019). After solvation, Na⁺ and Cl⁻ ions were inserted to neutralize the system. Then, the concentration of 150 mM NaCl was added to the systems and energy was optimized using the steepest descent method. The system was equilibrated by position restrained simulation in NPT and NVT ensemble phases when NPT defined as constant substance amount, pressure and temperature, and NVT defined as constant substance amount, volume and temperature. The equilibration was done for 1 ns at 310K and subsequently submitted for simulation for a total duration of 20 ns. In order to analyze the results, the atomic coordinates were recorded every 2 ps (Farasat et al., 2017).

The backbone root mean square deviation (RMSD) and root mean square fluctuation (RMSF) of the complexes were analyzed by the tools in GROMACS to understand the MD of each system. Finally, LigPlot software was used to analyze the hydrogen and hydrophobic interactions and the hydrogen bond lengths (Wallace et al., 1995).

3. Results

3.1. CD8+ T-cell epitope (class I) prediction

Based on defined HLA-I alleles (Table 1), epitope prediction programs predicted a number of different epitopes for each Fim antigen (Table S1, supplementary material). All selected epitopes were introduced to the clustering tools and accordingly the epitopes with similar amino acid sequences were placed in a unique cluster.

The prediction of epitope immunogenicity showed different scores for each epitope. Because all predicted epitopes showed some degrees of immunogenicity, none of them was

removed in this step. However, the immunogenicity scores were recorded and considered for the selecting of final epitopes where higher immunogenicity scores were assumed as a positive point. The immunogenicity scores of the final selected epitopes of each Fim antigen have been shown in Table 2.

3.2. CD4+ T-cell epitope (class II) prediction

To predict class-II epitopes, seven most frequent HLA-II alleles in the world population were obtained and prediction was performed based on these HLA-II alleles (Table 1). The clustering and selecting of the best epitopes were similar to those mentioned about class-I prediction (see section 3.1). IEDB and SYFPEITHI programs predicted a number of different epitopes for each Fim antigen while no epitopes with scores higher than threshold was found in ProPredII (Table S2, supplementary material).

IFN- γ production prediction showed different states (positive or negative) for each epitope. Since some epitopes predicted negative here had high prediction scores, we decided not to remove any epitope in this step. However, IFN- γ production states were recorded and considered for selecting the final epitopes where positivity for IFN- γ production was assumed as a positive point for epitope selection. The IFN- γ production states of the final selected epitopes of each Fim antigen are shown in Table 2.

3.3. Human similarity exclusion and searching experimental records

Following human similarity investigation, the number of epitopes was further reduced. The number of class-I epitopes after human similarity exclusion was as follow: 18, 27, 22, and 42, for FimA, FimF, FimG and FimH, respectively. The number of class-II epitopes after human similarity exclusion was as follow: 43, 43, 19, and 46, for FimA, FimF, FimG and FimH, respectively.

Using the IEDB and Pubmed, the selected epitopes and the whole antigens of Fim proteins were investigated. However, no experimental record was found for any of them, although there are some reports on Fim proteins for other bacteria from enterobacteriaceae family.

3.4. Finding class-II epitopes containing class-I epitopes

For each Fim protein, all class-I and II epitopes that had been selected in previous steps, were compared using cluster analysis tools. We found 11, 9, 13, and 12 clusters for FimA, FimF, FimG, and FimH, respectively. Each cluster contained at least one class-II and one class-I epitopes. These clusters were selected for further analysis.

3.5. Final selected T-cell epitopes

From remained clusters, final T-cell epitopes were selected based on the selection criteria as previously mentioned (Section 2.6). For each antigen, the selected epitopes were

Table 2. The top list of predicted epitopes.

Antigen	Windows of class II and I epitopes ^a	Class-II epitopes ^b				Class-I epitopes							
		Epitope	SYFPEITHI	IEDB	IFNg ^d	Docking	Epitope	Allele	SYFPEITHI	ProPredI	IEDB	Immunogenicity	Docking
FimA	KIKTLAMIVSALS	KIKTLAMIVSALS	10	6.4	-	-37.4	LAMIVSAL	HLA-B*35:01	12	N/A	0.2	0.04	-55.3
	TVQLGOVRSAKLATA	TVQLGOVRSAKLATA	18	6.2	+	-85.8	QLGOVRSAK	HLA-A*02:01	23	114	0.8	0.05	-70.1
	TAGIANADATFKVQY	TAGIANADATFKVQY	18	N/A	+	-98.7	IANDATFK	HLA-B*51:01	15	N/A	N/A	0.2	-82.9
	NITVLALONSAAGSA	NITVLALONSAAGSA	19	N/A	+	-76.9	LALONSAAG	HLA-B*35:01	N/A	N/A	0.5	-0.23	-57.9
FimF	GNPIPFQARYATG	GNPIPFQARYATG	24	0.68	-	-94.3	NIIPFQARY	HLA-A*01:01	17	10	N/A	0.1	-88.8
	MRTLQYLLGALFTLG	MRTLQYLLGALFTLG	14	6.4	-	-108	YLLGALFTL	HLA-A*02:01	32	4850	0.2	0.18	-92.2
	PAALAADSTIAISGY	PAALAADSTIAISGY	24	N/A	+	-75.1	LAADSTIAI	HLA-B*51:01	25	315	0.4	0.04	-55.3
	TSLLKLDAGTSAAG	TSLLKLDAGTSAAG	18	N/A	-	-75.7	SLLKLDAGT	HLA-A*02:01	22	28	N/A	-0.16	-84.6
FimG	QTNILNFYARLMATQ	QTNILNFYARLMATQ	28	0.69	+	-91.3	NILNFYARL	HLA-A*02:01	23	62	N/A	0.16	-89.3
	PFRIVLSPCGTSVTA	PFRIVLSPCGTSVTA	14	6.2	+	-94.8	SPCGTSVTA	HLA-B*51:01	15	13	N/A	-0.04	-84
	MKWTHVWGWLGLLT	MKWTHVWGWLGLLT	10	N/A	-	-120	KWTHVWGWL	HLA-A*02:01	14	11	0.5	0.3	-122
	GWLLAGLLTASASLR	GWLLAGLLTASASLR	18	N/A	+	-87.6	WLLAGLLTA	HLA-A*24:02	25	194	0.7	0.07	-79.3
FimH	AGLLTASASLRAADV	AGLLTASASLRAADV	24	6.4	+	-87.6	SASLRAADV	HLA-B*51:01	19	100	N/A	0.07	-79.8
	LRAADVTLTVNGKVV	LRAADVTLTVNGKVV	14	N/A	+	-81.3	RAADVTLTV	HLA-B*51:01	24	66	N/A	0.12	-87.2
	QGTIQAVINVTYYA	QGTIQAVINVTYYA	20	N/A	-	-85.4	AVINVTYY	HLA-A*02:01	13	N/A	N/A	0.13	-90.6
	KKIPLFTLLLLGW	KKIPLFTLLLLGW	34	5.7	-	-97.3	IPLFTLLLL	HLA-B*51:01	22	143	0.4	0.17	-80.8
FimI	ITAGSLI AVLILHOT	ITAGSLI AVLILHOT	10	N/A	-	-87.1	AGSLI AVLIL	HLA-B*51:01	18	88	N/A	0.13	-71.5
	SDSFQFIWNIYANNND	SDSFQFIWNIYANNND	22	6.8	-	-114	DSFQFIWNI	HLA-B*51:01	16	18	N/A	0.34	-116
	QTNINYNSDSFQFIWN	QTNINYNSDSFQFIWN	20	N/A	+	-72.8	YNSDSFQFI	HLA-B*51:01	15	N/A	N/A	-0.11	-111
	ARVIYDSRTDKPWPA	ARVIYDSRTDKPWPA	18	N/A	+	-100	VIYDSRTDK	HLA-A*03:01	25	N/A	0.24	-0.04	-72.2

^aCommon sequences of class-II and I epitopes are presented in this column. The class-I epitopes that are residing in the class-II epitopes are shown by bold underlined fonts.

^bAll class-II epitopes were restricted to HLA-DRB1*15:01 allele (not shown here).

^cFor SYFPEITHI and ProPredI the higher numbers show higher scores (cutoff were set on 10); for IEDB the lower numbers show higher scores (cutoff were set on 10 and 1 for class-II and class-I epitopes, respectively);

for immunogenicity the more positive numbers show more immunogen epitopes; for docking score the more negative numbers show peptides with higher binding affinity. N/A: not available.

^dPredicted negative and positive in IFNg production is shown by '-' and '+', respectively.

Table 3. The population coverage calculation results.

Class-II epitopes	Population/area	FimA			FimF			FimG			FimH		
		coverage ^a	average_hit ^b	pc90 ^c	coverage ^a	average_hit ^b	pc90 ^c	coverage ^a	average_hit ^b	pc90 ^c	coverage ^a	average_hit ^b	pc90 ^c
Argentina		30.80%	1.48	0.43	28.96%	1.47	0.59	28.96%	1.27	0.35	30.80%	1.38	0.58
Brazil		24.33%	1.17	0.4	23.30%	1.18	0.59	23.30%	0.97	0.36	24.33%	1.05	0.53
China		26.26%	1.27	0.41	24.99%	1.27	0.59	24.99%	1.15	0.36	26.26%	1.23	0.54
Colombia		20.35%	0.98	0.38	19.59%	0.99	0.58	19.59%	0.84	0.35	20.35%	0.9	0.5
Greece		35.40%	1.74	0.46	32.90%	1.69	0.58	32.90%	1.43	0.35	35.40%	1.6	0.62
Italy		68.08%	4.02	0.94	63.03%	3.32	0.78	63.03%	2.16	0.47	68.08%	2.94	1.25
United States		56.73%	3.05	0.69	48.94%	2.65	0.26	48.94%	2.29	0.15	56.73%	2.81	0.92
Average		37.42	1.96	0.53	34.53	1.8	0.57	34.53	1.44	0.34	37.42	1.7	0.71
Standard deviation		16.68	1.05	0.19	14.61	0.8	0.14	14.61	0.53	0.09	16.68	0.77	0.26
Class-I epitopes													
Population/area		coverage ^a	average_hit ^b	pc90 ^c	coverage ^a	average_hit ^b	pc90 ^c	coverage ^a	average_hit ^b	pc90 ^c	coverage ^a	average_hit ^b	pc90 ^c
Argentina		64.55%	2.52	0.28	56.96%	2.96	0.23	64.55%	2.66	0.28	56.96%	2.88	0.23
Brazil		74.45%	2.75	0.39	67.59%	3.45	0.31	74.45%	2.99	0.39	67.59%	3.21	0.31
China		76.55%	1.84	0.43	74.80%	2.47	0.4	76.55%	2.24	0.43	74.80%	3.42	0.4
Colombia		8.22%	0.33	0.44	8.22%	0.41	0.54	8.22%	0.41	0.54	8.22%	0.41	0.54
Italy		91.95%	4.63	1.28	84.78%	5.28	0.66	91.95%	4.42	1.2	84.78%	4.64	0.66
United States		86.33%	3.54	0.73	81.85%	4.61	0.55	86.33%	3.89	0.73	81.85%	4.36	0.55
Average		67.01	2.6	0.59	62.37	3.2	0.45	67.01	2.77	0.59	62.37	3.15	0.45
Standard deviation		27.7	1.34	0.34	25.9	1.57	0.15	27.7	1.28	0.3	25.9	1.37	0.15

^aProjected population coverage.^bAverage number of epitope hits/HLA combinations recognized by the population.^cMinimum number of epitope hits/HLA combinations recognized by 90% of the population.

Table 4. The selected epitopes for MD simulation studies.

Epitope class	Selected epitope	Epitope symbol	Antigen	HLA no. ^a	Selected HLA ^b	HLA symbol	Best prediction score ^c	IFN γ ^d	Immunogenicity	Docking score
Class-II	AGLLTASASLRAADV	EIIG1	FimG	5	HLA-DRB1*15:01	D15	26	+	N/A	-87.6
Internal class-I	SASLRAADV	EG5	FimG	4	HLA-B*51:01	B51	19	N/A	0.07	-79.8

^aNumber of HLA that recognized this epitope.

^bThe selected HLA that serves as receptor in MD simulation studies.

^cThe best prediction score achieved by the epitope (in SYFPEITHI tool).

^dPredicted positive in IFN γ production is shown by '+'.
N/A: not available.

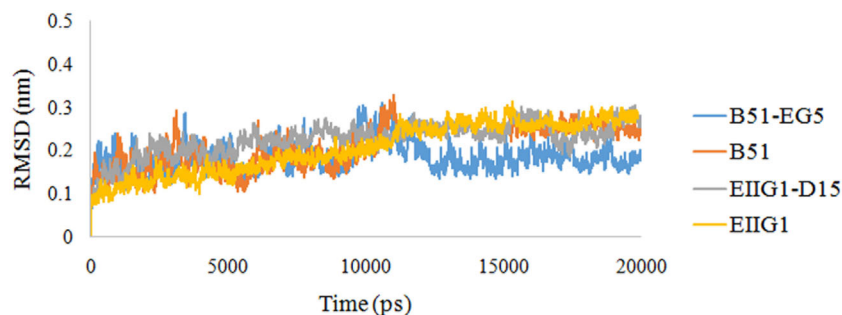


Figure 1. RMSD values of the receptors during MD simulation with the GROMACS version 5.1. The RMSD values (nm) of the B51 and D15 receptors alone and in combination with their ligand (epitopes) are shown by different colors.

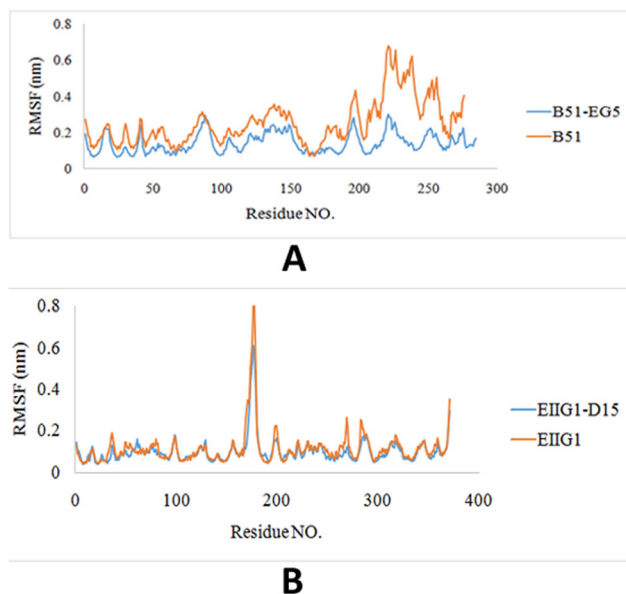


Figure 2. RMSF values of the receptors and ligands during MD simulation with the GROMACS version 5.1. (A) The RMSF values (nm) of the B51 receptor alone and in combination with its ligand (epitope). (B) The RMSF values (nm) of the D15 receptor alone and in combination with its ligand (epitope).

composed of five class-II epitopes each contains one class-I epitope (Table 2). Note that each selected epitope was restricted to more than one HLA allele (Table S3, supplementary material), however to make the issue simple and docking feasibility only one allele was chosen for each epitope. These epitopes were evaluated by molecular docking.

3.6. Prediction of population coverage

Seven countries with Carbapenemase-producing *K. pneumoniae* were used for population coverage analysis. For selected countries, the population coverage was predicted based on

the final epitopes of each antigen and their restricted alleles. The results showed that the predicted class-I and II epitopes theoretically cover ~35% and ~65% (in average) of the populations studied, respectively (Table 3).

3.7. Tertiary structure prediction and molecular docking

The 3D structures of HLA alleles were directly downloaded from PDB data bank and the tertiary structures of the final epitopes were modeled by PEP-FOLD server. Evaluations of models by Ramachandran plot showed that high percentages of the amino acid residues of the models were located in the favored regions that indicates the high quality of the models (plots are not shown).

Using HADDOCK server, the molecular docking scores of HLA-I and II in combination with their epitopes for each Fim antigen were determined (Table 2).

3.8. MD simulation analysis

The selected class-II epitope for MD studies was AGLLTASASLRAADV from FimG antigen that contains an internal class-I epitope (underlined). This class-II epitope had a low docking score (high affinity) of -87.6, recognized by five HLA-II alleles, had the best prediction score of 26 (by SYFPEITHI), and was predicted positive in IFN- γ production. Similarly, its internal class-I epitope had a low docking score (high affinity) of -79.8, recognized by four HLA-I alleles, had the best prediction score of 19 (by SYFPEITHI), and had immunogenicity score of 0.07 (Table 4).

To accurately evaluate the stability and binding state of epitope-HLA (ligand-receptor) complexes, MD simulation was performed for a total duration of 20 ns. For easy explanations of MD results, symbols were used for the receptors and the epitopes (as Table 4).

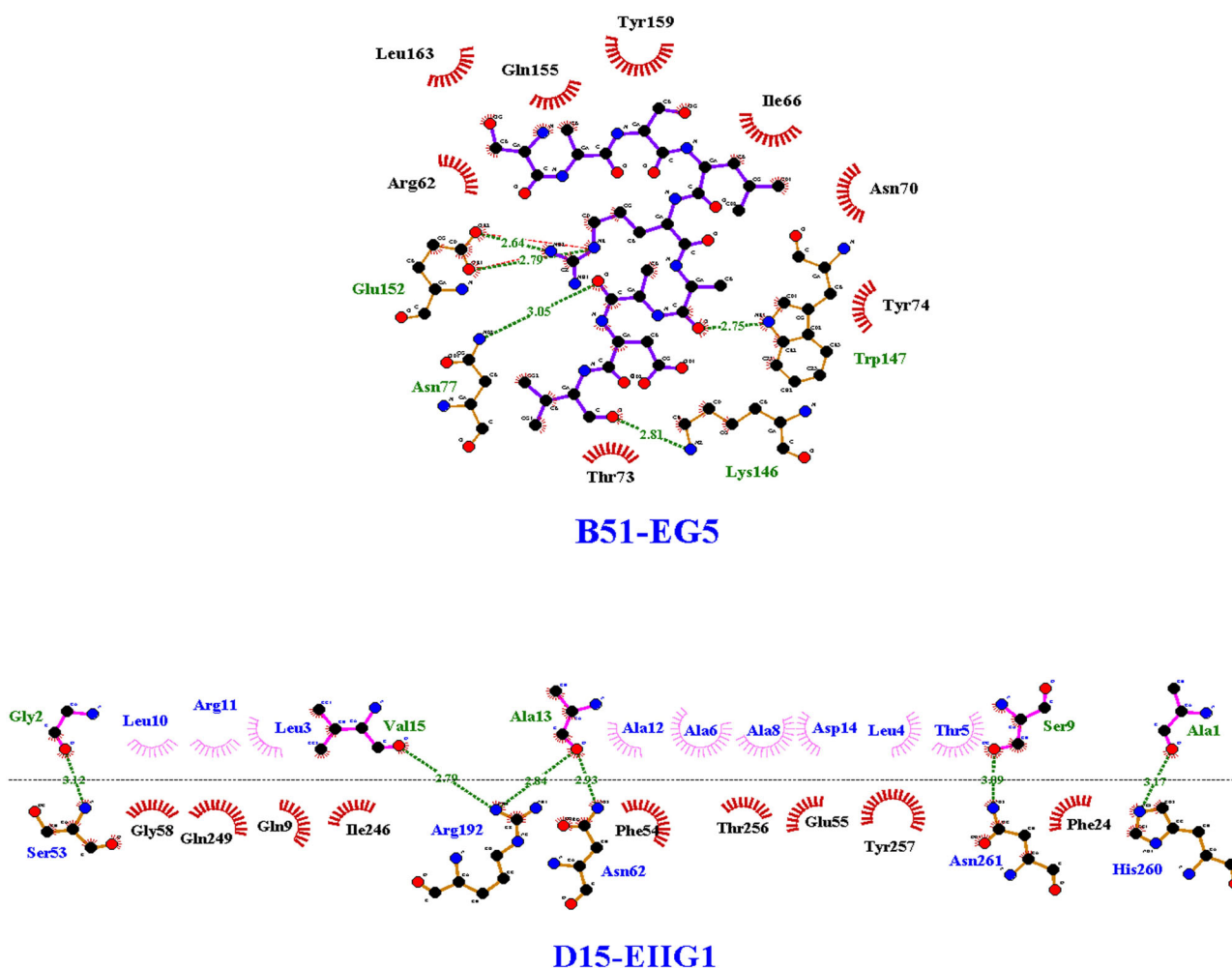


Figure 3. Hydrophobic and hydrogen bond forming residues in the best docked conformations. The receptor amino acids residues involved in H-bond and hydrophobic interactions with ligand residues are shown. Half circle in red color indicates the residues involved in hydrophobic interactions. Hydrogen bonds are shown with green dotted lines. The length of each hydrogen bond is shown as number on each bond.

RMSD is an essential parameter which is applied to predict the system equilibration during the simulation (Kaur et al., 2019). RMSD profiles were calculated for backbone amino acid residues of the receptors to accomplish the system dynamical stability. As shown in Figure 1, the receptor D15 and B51 alone and in combination with EIIG1 and EG5 epitopes, reached stability after approximately 11 ns.

RMSF value provides a better understanding of the protein flexibility and structural fluctuations (Chen et al., 2016; Mahapatra et al., 2018). To define the flexible regions of the B51 and D15 in the complexes, the RMSF of their $C\alpha$ atoms were evaluated. The RMSF values of the two complexes of D15–EIIG1 and B51–EG5 are shown in Figure 2. The B51 protein reached the highest flexibility in 220–230 amino acid residues (Figure 2(a)) and D15 protein showed the highest flexibility in 190–199 amino acid residues (Figure 2(b)).

The residues involved in the hydrophobic interactions and hydrogen bonds were investigated by extracting the PDB file of MD simulation from GROMACS software and its graphically evaluation by LigPlot program. The residues involved in hydrophobic interactions and the hydrogen bonds as well as the hydrogen bonds lengths in the complexes have been shown in Figure 3 and Table S4 (supplementary material).

4. Discussion

The control of *K. pneumoniae* infections is a complicated issue due to the increasing resistance to various antibiotics and having virulence factors such as endotoxins inducing septic shock, capsular polysaccharide inhibiting phagocytosis and complement-mediated killing (Kim et al., 2002; Merino et al., 1992; Podschun & Ullmann, 1998). Immunotherapy treatment and vaccination seem promising alternatives to control infections caused by *K. pneumoniae* (Ahmad et al., 2012).

Here we studied four *K. pneumoniae* type 1 fimbriae antigens. There is no publically available *in vivo*, *in vitro*, or *in silico* studies on vaccination against these proteins in the literature. Therefore, our *in silico* study would be assumed as the first study to characterize these proteins and find their probable T-cell specific epitopes. It is noteworthy that there are some *in silico* studies on other *K. pneumoniae* proteins as vaccine candidates, such as type 3 fimbriae proteins (Li et al., 2010), outer membrane proteins (Farhadi et al., 2015), and whole cell proteins (Dar et al., 2019). These studies found several vaccine candidates for *K. pneumoniae*, characterized them, and predicted their T-cell and B-cell epitopes.

Innate and acquired immunity (both humoral and cell-dependent) are important to control infections of *K. pneumoniae*. In our study the T-cell-specific epitopes as main immunogen parts of the Fim antigens were found using different prediction tools. For each antigen, a large number of epitopes were predicted. These epitopes should be reduced into a manageable numbers. Therefore, here we applied some analyses to limit the number of epitopes and find the best ones including the selection of epitopes with higher prediction scores, prediction by several tools, and non-similarity to human peptides. After reduction the numbers of epitope, other parameters were applied to select the most immunogenic T-cell-specific epitopes including immunogenicity (for class-I epitopes), IFN- γ production (for class-II epitopes), and binding affinity to HLA molecules through molecular docking approaches (for both class-I and II). These analyses led to introducing five class-II, and five class-I T-cell epitopes for each antigen which are highly immunogenic, non-similar to human peptides, and bind with high affinity to their HLAs. All class-II epitopes selected here contained at least one immunogenic class-I epitope. If these epitopes use as vaccines and process well by proteases, they may result in the both class-I and II epitopes exposed by MHC class I and II that consequently induce both CD4+ and CD8+ specific responses.

Moreover, the final selected T-cell epitopes predicted here showed to cover a large percentage of the human population. The population coverage was estimated by IEDB analysis tool that calculates the average hit, coverage, and pc90 which are defined as the average number of HLA-epitope combinations recognized by the population, the projected population coverage, and the minimum number of HLA-epitope combinations recognized by 90 percent of the population, respectively (Bui et al., 2006). In the present study, the average hit, coverage, and pc90 scores were high suggesting that our predicted epitopes can be used to vaccinate a large number of human populations. Note that the population coverage predicted for class-I epitopes cover the higher percentage compared to class-II epitopes that may refer to the fact that only a few of our HLA-II alleles presented in the population coverage tool and our HLA-II alleles are less frequent in the seven countries selected in our study.

None of our predicted epitopes found in the previous experimental records which may be due to the limited experimental studies on *K. pneumoniae* and more apparently on Fim antigens. The inadequately experimental records on *K. pneumoniae* make a serious limitation for validation of epitope predicted via *in silico* approaches.

It has been recommended to use multiple prediction methods to improve the overall prediction performance (Trost et al., 2007). Here we used three different tools to predict both class I and II T-cell-specific epitopes namely IEDB, SYFPEITHI, and ProPred (I or II).

SYFPEITHI employs a log-based score (Rammensee et al., 1999), ProPredI uses HLA half time dissociation and few other matrices (Singh & Raghava, 2001; 2003), and IEDB apply consensus method consisting of stabilized matrix

method (SMM), artificial neural network (ANN), and combinatorial peptide libraries (Comlib) algorithms (Fleri et al., 2017).

To choose the most desirable epitopes, the cutoff scores of SYFPEITHI and ProPred were set on ≥ 10 score. The cutoff score setting is generally depends on the investigator's decision (Duarte et al., 2015). Therefore, regarding our previous work (Akya et al., 2019) we assume the epitopes picked out at the cutoff scores defined here are energetically best fitted to HLA binding grooves. For IEDB tools the cutoff scores were ≤ 1 percentile rank for class-I and ≤ 20 percentile rank for class-II epitope prediction. These cutoff scores were chosen based on IEDB recommendations (Fleri et al., 2017) which presumably optimized for epitope selection.

The MD simulation study has an important role in the recognition of interactions between receptors and ligands as well as receptors conformational modifications at the atomic level. Results obtained via MD simulation studies provide a better view of understanding the binding state and dynamics of the receptor-ligand combination (Bello & Correa-Basurto, 2013; Knapp et al., 2015; Mirza et al., 2016; Singaravelu et al., 2014).

In our study, MD simulation was performed for the best class-II epitope and its internal class-I epitope in combination with their receptors (HLA molecules). The results, which are presented by RMSD and RMSF values of the complexes, indicated the system stability with the minimum possible deviation. It means that both selected epitopes of the present study are favorable candidates for stably binding to HLA molecules.

Altogether, our results suggested that the final T-cell-specific epitopes can be applied in vaccine development against *K. pneumoniae*. However, although *in silico* approaches might identify potent epitopes as vaccine candidates with highly immunogenicity and broad protection, whether these candidates can be successfully produce effective vaccines need to be tested via *in vitro* and *in vivo* studies.

Acknowledgements

The supported of this work by Infectious Diseases Research Center of Kermanshah University of Medical Sciences and Clinical Research Development Center of Imam Reza Hospital is highly appreciated.

Disclosure statement

No potential conflicts of interest we disclosed.

Funding

This research was financially supported by the Kermanshah University of Medical Sciences.

Credit authorship contribution statement

Mosayeb Rostamian: Conceptualization, methodology, data curation, writing – review and editing.

Alireza Farasat: Methodology, data curation, roles/writing – original draft.

Roya Chegene Lorestani: Data curation, software.

Fatemeh Nemati Zargaran: Data curation, software.

Keyghobad Ghadiri: Funding acquisition, resources.

Alisha Akya: Project administration, supervision, writing – review and editing.

ORCID

Mosayeb Rostamian  <http://orcid.org/0000-0002-1071-7019>

References

- Ahmad, T. A., El-Sayed, L. H., Haroun, M., Hussein, A. A., & El Ashry, E. S. H. (2012). Development of immunization trials against *Klebsiella pneumoniae*. *Vaccine*, 30(14), 2411–2420. <https://doi.org/10.1016/j.vaccine.2011.11.027>
- Akya, A., Farasat, A., Ghadiri, K., & Rostamian, M. (2019). Identification of HLA-I restricted epitopes in six vaccine candidates of *Leishmania tropica* using immunoinformatics and molecular dynamics simulation approaches. *Infection, Genetics and Evolution: Journal of Molecular Epidemiology and Evolutionary Genetics in Infectious Diseases*, 75, 103953. <https://doi.org/10.1016/j.meegid.2019.103953>
- Babu, L., Uppalapati, S. R., Sripathy, M. H., & Reddy, P. N. (2017). Evaluation of recombinant multi-epitope outer membrane protein-based *Klebsiella pneumoniae* subunit vaccine in mouse model. *Frontiers in Microbiology*, 8, 1805. <https://doi.org/10.3389/fmicb.2017.01805>
- Bai, Q., & Yao, X. (2016). Investigation of allosteric modulation mechanism of metabotropic glutamate receptor 1 by molecular dynamics simulations, free energy and weak interaction analysis. *Scientific Reports*, 6, 21763. <https://doi.org/10.1038/srep21763>
- Bello, M., & Correa-Basurto, J. (2013). Molecular dynamics simulations to provide insights into epitopes coupled to the soluble and membrane-bound MHC-II complexes. *PLoS One*, 8(8), e72575. <https://doi.org/10.1371/journal.pone.0072575>
- Bui, H. H., Sidney, J., Dinh, K., Southwood, S., Newman, M. J., & Sette, A. (2006). Predicting population coverage of T-cell epitope-based diagnostics and vaccines. *BMC Bioinformatics*, 7, 153. <https://doi.org/10.1186/1471-2105-7-153>
- Calis, J. J. A., Maybeno, M., Greenbaum, J. A., Weiskopf, D., De Silva, A. D., Sette, A., Keşmir, C., & Peters, B. (2013). Properties of MHC class I presented peptides that enhance immunogenicity. *PLoS Computational Biology*, 9(10), e1003266. <https://doi.org/10.1371/journal.pcbi.1003266>
- Chen, J., Wang, J., & Zhu, W. (2016). Molecular mechanism and energy basis of conformational diversity of antibody SPE7 revealed by molecular dynamics simulation and principal component analysis. *Scientific Reports*, 6, 36900. <https://doi.org/10.1038/srep36900>
- Choi, M., Tennant, S. M., Simon, R., & Cross, A. S. (2019). Progress towards the development of *Klebsiella* vaccines. *Expert Review in Vaccines*, 18(7), 681–691. <https://doi.org/10.1080/14760584.2019.1635460>
- Chyau Liang, T. (1998). *Encyclopedia of immunology* (2nd ed.). Elsevier Ltd. <https://doi.org/10.1006/rwei.1999.0219>
- Dar, H. A., Zaheer, T., Shehroz, M., Ullah, N., Naz, K., Muhammad, S. A., Zhang, T., & Ali, A. (2019). Immunoinformatics-aided design and evaluation of a potential multi-epitope vaccine against *Klebsiella pneumoniae*. *Vaccines*, 7(3), 88. <https://doi.org/10.3390/vaccines7030088>
- de Vries, S. J., & Bonvin, A. M. J. J. (2011). CPOR: A consensus interface predictor and its performance in prediction-driven docking with HADDOCK. *PLoS One*, 6(3), e17695. <https://doi.org/10.1371/journal.pone.0017695>
- Dominguez, C., Boelens, R., & Bonvin, A. M. J. J. (2003). HADDOCK: A protein-protein docking approach based on biochemical or biophysical information. *Journal of the American Chemical Society*, 125(7), 1731–1737. <https://doi.org/10.1021/ja026939x>
- Duarte, A., Queiroz, A. T. L., Tosta, R., Carvalho, A. M., Barbosa, C. H., Bellio, M., de Oliveira, C. I., & Barral-Netto, M. (2015). Prediction of CD8+ epitopes in *Leishmania braziliensis* proteins using EPIBOT: *In silico* search and *in vivo* validation. *PLoS One*, 10(4), e0124786. <https://doi.org/10.1371/journal.pone.0124786>
- Farasat, A., Rahbarizadeh, F., Hosseinzadeh, G., Sajjadi, S., Kamali, M., & Keihan, A. H. (2017). Affinity enhancement of nanobody binding to EGFR: *In silico* site-directed mutagenesis and molecular dynamics simulation approaches. *Journal of Biomolecular Structure and Dynamics*, 35(8), 1710–1728. <https://doi.org/10.1080/07391102.2016.1192065>
- Farhadi, T., Nezafat, N., Ghasemi, Y., Karimi, Z., Hemmati, S., & Erfani, N. (2015). Designing of complex multi-epitope peptide vaccine based on Omeps of *Klebsiella pneumoniae*: An *in silico* approach. *International Journal of Peptide Research and Therapeutics*, 21(3), 325–341. <https://doi.org/10.1007/s10989-015-9461-0>
- Fleri, W., Paul, S., Dhanda, S. K., Mahajan, S., Xu, X., Peters, B., & Sette, A. (2017). The immune epitope database and analysis resource in epitope discovery and synthetic vaccine design. *Frontiers in Immunology*, 8, 278. <https://doi.org/10.3389/fimmu.2017.00278>
- Gfeller, D., Guillaume, P., Michaux, J., Pak, H.-S., Daniel, R. T., Racle, J., Coukos, G., & Bassani-Sternberg, M. (2018). The length distribution and multiple specificity of naturally presented HLA-I ligands. *Journal of Immunology*, 201(12), 3705–3716. <https://doi.org/10.4049/jimmunol.1800914>
- Gheibi, N., Ghorbani, M., Shariatifar, H., & Farasat, A. (2019). *In silico* assessment of human calprotectin subunits (S100A8/A9) in presence of sodium and calcium ions using molecular dynamics simulation approach. *PLoS One*, 14(10), e0224095. <https://doi.org/10.1371/journal.pone.0224095>
- Gheibi, N., Ghorbani, M., Shariatifar, H., & Farasat, A. (2020). Effects of unsaturated fatty acids (arachidonic/oleic acids) on stability and structural properties of calprotectin using molecular docking and molecular dynamics simulation approach. *PLoS One*, 15(3), e0230780. <https://doi.org/10.1371/journal.pone.0230780>
- Gonzalez-Galarza, F. F., Takeshita, L. Y., Santos, E. J., Kempson, F., Maia, M. H., da Silva, A. L., Teles e Silva, A. L., Ghattaoraya, G. S., Alfirevic, A., Jones, A. R., & Middleton, D. (2015). Allele frequency net 2015 update: New features for HLA epitopes, KIR and disease and HLA adverse drug reaction associations. *Nucleic Acids Research*, 43(Database issue), D784–D788. <https://doi.org/10.1093/nar/gku1166>
- Kaur, G., Pandey, B., Kumar, A., Garewal, N., Grover, A., & Kaur, J. (2019). Drug targeted virtual screening and molecular dynamics of LipU protein of *Mycobacterium tuberculosis* and *Mycobacterium leprae*. *Journal of Biomolecular Structure and Dynamics*, 37(5), 1254–1269. <https://doi.org/10.1080/07391102.2018.1454852>
- Kazi, A., Chuah, C., Majeed, A. B. A., Leow, C. H., Lim, B. H., & Leow, C. Y. (2018). Current progress of immunoinformatics approach harnessed for cellular- and antibody-dependent vaccine design. *Pathogens and Global Health*, 112(3), 123–131. <https://doi.org/10.1080/20477724.2018.1446773>
- Kim, Y.-K., Pai, H., Lee, H.-J., Park, S.-E., Choi, E.-H., Kim, J., Kim, J.-H., & Kim, E.-C. (2002). Bloodstream infections by extended-spectrum beta-lactamase-producing *Escherichia coli* and *Klebsiella pneumoniae* in children: Epidemiology and clinical outcome. *Antimicrobial Agents and Chemotherapy*, 46(5), 1481–1491. <https://doi.org/10.1128/AAC.46.5.1481-1491.2002>
- Knapp, B., Demharter, S., Esmailbeiki, R., & Deane, C. M. (2015). Current status and future challenges in T-cell receptor/peptide/MHC molecular dynamics simulations. *Briefings in Bioinformatics*, 16(6), 1035–1044. <https://doi.org/10.1093/bib/bbv005>
- Lavender, H., Jagnow, J. J., & Clegg, S. (2005). *Klebsiella pneumoniae* type 3 fimbria-mediated immunity to infection in the murine model of respiratory disease. *International Journal of Medical Microbiology: IJMM*, 295(3), 153–159. <https://doi.org/10.1016/j.ijmm.2005.04.001>
- Lee, W. H., Il Choi, H., Hong, S. W., Kim, K. S., Gho, Y. S., & Jeon, S. G. (2015). Vaccination with *Klebsiella pneumoniae*-derived extracellular vesicles protects against bacteria-induced lethality via both humoral and cellular immunity. *Experimental Molecular Medicine*, 47, e183. <https://doi.org/10.1038/emm.2015.59>
- Li, W., Cowley, A., Uludag, M., Gur, T., McWilliam, H., Squizzato, S., Park, Y. M., Buso, N., & Lopez, R. (2015). The EMBL–EBI bioinformatics web and programmatic tools framework. *Nucleic Acids Research*, 43(W1), W580–W584. <https://doi.org/10.1093/nar/gkv279>
- Li, Y., Jie Li, Z., Yu Han, W., Cheng Lei, L., Jiang Sun, C., Feng, X., Tao Du, C., Feng Du, T., & Min Gu, J. (2010). Identification and characterization of Th cell epitopes in MrkD adhesin of *Klebsiella pneumoniae*.

- Microbial Pathogenesis*, 49(1–2), 8–13. <https://doi.org/10.1016/j.mic-path.2010.03.009>
- Lovell, S. C., Davis, I. W., Arendall, W. B., de Bakker, P. I. W., Word, J. M., Prisant, M. G., Richardson, J. S., & Richardson, D. C. (2003). Structure validation by Calpha geometry: Phi, psi and Cbeta deviation. *Proteins: Structure, Function, and Bioinformatics*, 50(3), 437–450. <https://doi.org/10.1002/prot.10286>
- Dikhit, M. Y., Ansari, V., Kalyani, R., Mansuri, B. R., Sahoo, B., Dehury, A., Amit, R. K., Topno, G. C., Sahoo, V., Ali, S., Bimal, P., & Das, (2016). Computational prediction and analysis of potential antigenic CTL epitopes in Zika virus: A first step towards vaccine development. *Infection Genetics & Evolution*, 45, 187–197. <https://doi.org/10.1016/j.meegid.2016.08.037>
- Mahapatra, M. K., Bera, K., Singh, D. V., Kumar, R., & Kumar, M. (2018). *In silico* modelling and molecular dynamics simulation studies of thiazolidine based PTP1B inhibitors. *Journal of Biomolecular Structure and Dynamics*, 36(5), 1195–1211. <https://doi.org/10.1080/07391102.2017.1317026>
- Malathi, K., Anbarasu, A., & Ramaiah, S. (2019). Identification of potential inhibitors for *Klebsiella pneumoniae* carbapenemase-3: A molecular docking and dynamics study. *Journal of Biomolecular Structure and Dynamics*, 37(17), 4601–4613. <https://doi.org/10.1080/07391102.2018.1556737>
- Merino, S., Camprubi, S., Alberti, S., Benedi, V. J., & Tomas, J. M. (1992). Mechanisms of *Klebsiella pneumoniae* resistance to complement-mediated killing. *Infection and Immunity*, 60(6), 2529–2535. <https://doi.org/10.1128/IAI.60.6.2529-2535.1992>
- Miryala, S. K., Anbarasu, A., & Ramaiah, S. (2018). Discerning molecular interactions: A comprehensive review on biomolecular interaction databases and network analysis tools. *Gene*, 642, 84–94. <https://doi.org/10.1016/j.gene.2017.11.028>
- Miryala, S. K., Anbarasu, A., & Ramaiah, S. (2020). Role of SHV-11, a class A β -lactamase, gene in multidrug resistance among *Klebsiella pneumoniae* strains and understanding its mechanism by gene network analysis. *Microbiological Drug Resistance*, 26(8), 900–908. <https://doi.org/10.1089/mdr.2019.0430>
- Mirza, M. U., Rafique, S., Ali, A., Munir, M., Ikram, N., Manan, A., Salo-Ahen, O. M. H., & Idrees, M. (2016). Towards peptide vaccines against Zika virus: Immunoinformatics combined with molecular dynamics simulations to predict antigenic epitopes of Zika viral proteins. *Scientific Reports*, 6, 37313. <https://doi.org/10.1038/srep37313>
- Munoz-Price, L. S., Poirel, L., Bonomo, R. A., Schwaber, M. J., Daikos, G. L., Cormican, M., Cornaglia, G., Garau, J., Gniadkowski, M., Hayden, M. K., Kumarasamy, K., Livermore, D. M., Maya, J. J., Nordmann, P., Patel, J. B., Paterson, D. L., Pitout, J., Villegas, M. V., Wang, H., Woodford, N., & Quinn, J. P. (2013). Clinical epidemiology of the global expansion of *Klebsiella pneumoniae* carbapenemases. *The Lancet: Infectious Diseases*, 13(9), 785–796. [https://doi.org/10.1016/S1473-3099\(13\)70190-7](https://doi.org/10.1016/S1473-3099(13)70190-7)
- Paczosa, M. K., & Meccas, J. (2016). *Klebsiella pneumoniae*: Going on the offense with a strong defense. *Microbiology. Molecular Biological Review*, 80(3), 629–661. <https://doi.org/10.1128/MMBR.00078-15>
- Panahi, H. A., Bolhassani, A., Javadi, G., & Noormohammadi, Z. (2018). A comprehensive *in silico* analysis for identification of therapeutic epitopes in HPV16, 18, 31 and 45 oncoproteins. *PLoS One*, 13(10), e0205933. <https://doi.org/10.1371/journal.pone.0205933>
- Piperaki, E. T., Syrogiannopoulos, G. A., Tzouveleki, L. S., & Daikos, G. L. (2017). *Klebsiella pneumoniae*: Virulence, biofilm and antimicrobial resistance. *The Pediatric Infectious Disease Journal*, 36(10), 1002–1005. <https://doi.org/10.1097/INF.0000000000001675>
- Podschun, R., & Ullmann, U. (1998). *Klebsiella* spp. as nosocomial pathogens: Epidemiology, taxonomy, typing methods, and pathogenicity factors. *Clinical Microbiology Reviews*, 11(4), 589–603. <https://doi.org/10.1128/CMR.11.4.589>
- Prasasty, V. D., Grazzolie, K., Rosmalena, R., Yazid, F., Ivan, F. X., & Sinaga, E. (2019). Peptide-based subunit vaccine design of T- and B-cells multi-epitopes against Zika virus using immunoinformatics approaches. *Microorganisms*, 7(8), 226. <https://doi.org/10.3390/microorganisms7080226>
- Rammensee, H., Bachmann, J., Emmerich, N. P., Bachor, O. A., & Stevanovic, S. (1999). SYFPEITHI: Database for MHC ligands and peptide motifs. *Immunogenetics*, 50(3–4), 213–219. <http://www.ncbi.nlm.nih.gov/pubmed/10602881>. <https://doi.org/10.1007/s002510050595>
- Rappuoli, R., Bottomley, M. J., D'Oro, U., Finco, O., & De Gregorio, E. (2016). Reverse vaccinology 2.0: Human immunology instructs vaccine antigen design. *The Journal of Experimental Medicine*, 213(4), 469–481. <https://doi.org/10.1084/jem.20151960>
- Schuler, M. M., Nastke, M. D., & Stevanovic, S. (2007). SYFPEITHI: Database for searching and T-cell epitope prediction. *Methods in Molecular Biology*, 409, 75–93. <http://www.ncbi.nlm.nih.gov/pubmed/18449993>. https://doi.org/10.1007/978-1-60327-118-9_5
- Shen, Y., Maupetit, J., Derreumaux, P., & Tuffery, P. (2014). Improved PEP-FOLD approach for peptide and miniprotein structure prediction. *Journal of Chemical Theory and Computation*, 10(10), 4745–4758. <https://doi.org/10.1021/ct500592m>
- Shon, A. S., Bajwa, R. P. S., & Russo, T. A. (2013). Hypervirulent (hyper-mucoviscous) *Klebsiella pneumoniae*: A new and dangerous breed. *Virulence*, 4(2), 107–118. <https://doi.org/10.4161/viru.22718>
- Singaravelu, M., Selvan, A., & Anishetty, S. (2014). Molecular dynamics simulations of lectin domain of FimH and immunoinformatics for the design of potential vaccine candidates. *Computation Biology and Chemistry*, 52, 18–24. <https://doi.org/10.1016/j.compbiolchem.2014.08.002>
- Singh, H., & Raghava, G. P. (2001). ProPred: Prediction of HLA-DR binding sites. *Bioinformatics (Oxford, England)*, 17(12), 1236–1237. <http://www.ncbi.nlm.nih.gov/pubmed/11751237>. <https://doi.org/10.1093/bioinformatics/17.12.1236>
- Singh, H., & Raghava, G. P. S. (2003). ProPred1: Prediction of promiscuous MHC Class-I binding sites. *Bioinformatics*, 19(8), 1009–1014. <http://www.ncbi.nlm.nih.gov/pubmed/12761064>. <https://doi.org/10.1093/bioinformatics/btg108>
- Staniszewska, M., Witkowska, D., & Gamian, A. (2000). [Fimbriae as a pathologic factor of bacteria and a carrier in conjugate vaccines]. *Postepy Higieny I Medycyny Doswiadczalnej*, 54, 727–747.
- Sugumar, M., Kumar, K. M., Manoharan, A., Anbarasu, A., & Ramaiah, S. (2014). Detection of OXA-1 β -lactamase gene of *Klebsiella pneumoniae* from blood stream infections (BSI) by conventional PCR and *in-silico* analysis to understand the mechanism of OXA mediated resistance. *PLoS One*, 9(3), e91800. <https://doi.org/10.1371/journal.pone.0091800>
- Swetha, R. G., Sandhya, M., Ramaiah, S., & Anbarasu, A. (2016). Identification of CD4+ T-cell epitope and investigation of HLA distribution for the immunogenic proteins of *Burkholderia pseudomallei* using *in silico* approaches: A key vaccine development strategy for melioidosis. *Journal of Theoretical Biology*, 400, 11–18. <https://doi.org/10.1016/j.jtbi.2016.04.009>
- Thevenet, P., Shen, Y., Maupetit, J., Guyon, F., Derreumaux, P., & Tuffery, P. (2012). PEP-FOLD: An updated de novo structure prediction server for both linear and disulfide bonded cyclic peptides. *Nucleic Acids Research*, 40(Web Server Issue), W288–W293. <https://doi.org/10.1093/nar/gks419>
- Trost, B., Bickis, M., & Kusaliik, A. (2007). Strength in numbers: Achieving greater accuracy in MHC-I binding prediction by combining the results from multiple prediction tools. *Immunome Research*, 3, 5. <https://doi.org/10.1186/1745-7580-3-5>
- van Zundert, G. C. P., Rodrigues, J. P. G. L. M., Trellet, M., Schmitz, C., Kastiris, P. L., Karaca, E., Melquiond, A. S. J., van Dijk, M., de Vries, S. J., & Bonvin, A. M. J. J. (2016). The HADDOCK2.2 web server: User-friendly integrative modeling of biomolecular complexes. *Journal of Molecular Biology*, 428(4), 720–725. <https://doi.org/10.1016/j.jmb.2015.09.014>
- Volkan, E., Kalas, V., & Hultgren, S. (2014). Pili and fimbriae of gram-negative bacteria. In Tang Y., Sussman M., Liu D., Poxton I., & Schwartzman J. (Eds.), *Molecular microbial microbiology* (2nd ed., pp. 147–162). Elsevier Ltd. <https://doi.org/10.1016/B978-0-12-397169-2.00008-1>
- Wallace, A. C., Laskowski, R. A., & Thornton, J. M. (1995). LIGPLOT: A program to generate schematic diagrams of protein–ligand interactions. *Protein Engineering*, 8(2), 127–134. <http://www.ncbi.nlm.nih.gov/pubmed/7630882>. <https://doi.org/10.1093/protein/8.2.127>
- Witkowska, D., Mieszala, M., Gamian, A., Staniszewska, M., Czarny, A., Przondo-Mordarska, A., Jaquinod, M., & Forest, E. (2005). Major structural proteins of type 1 and type 3 *Klebsiella* fimbriae are effective protein carriers and immunogens in conjugates as revealed from their immunological characterization. *FEMS Immunology and Medical Microbiology*, 45(2), 221–230. <https://doi.org/10.1016/j.femsim.2005.04.005>